Theses and Dissertations   1. Thesis and Dissertation Collection, all items

1996-03

Swell propagation across a wide continental shelf

Hendrickson, Eric J.

Monterey, California. Naval Postgraduate School

https://hdl.handle.net/10945/32160

NAVAL POSTGRADUATE SCHOOL
MONTEREY, CALIFORNIA

THESIS

SWELL PROPAGATION ACROSS A WIDE
CONTINENTAL SHELF

by

Eric J Hendrickson

March, 1996

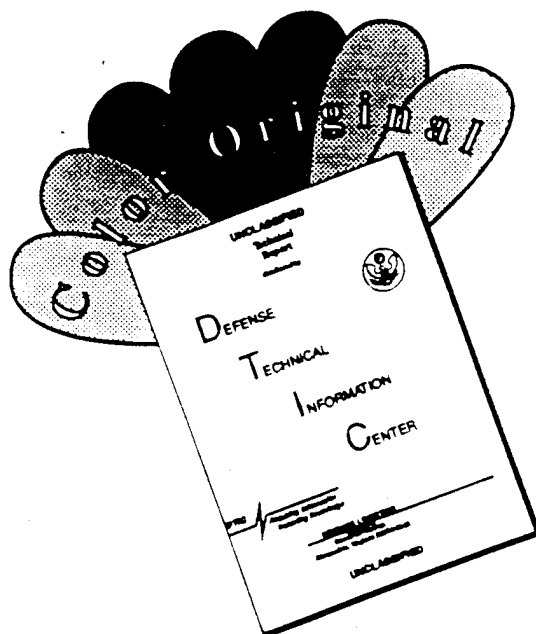Thesis Advisor: T.H.C. Herbers
Co-Advisor: W. C. O'Reilly

Approved for public release; distribution is unlimited.

19960708 021

DISCLAIMER NOTICE

THIS DOCUMENT IS BEST QUALITY AVAILABLE. THE COPY FURNISHED TO DTIC CONTAINED A SIGNIFICANT NUMBER OF COLOR PAGES WHICH DO NOT REPRODUCE LEGIBLY ON BLACK AND WHITE MICROFICHE.

REPORT DOCUMENTATION PAGE			Form Approved OMB No. 0704-

Public reporting burden for this collection of information is estimated to average 1 hour per response, including the time for reviewing instruction, searching existing data sources, gathering and maintaining the data needed, and completing and reviewing the collection of information. Send comments regarding this burden estimate or any other aspect of this collection of information, including suggestions for reducing this burden, to Washington Headquarters Services, Directorate for Information Operations and Reports, 1215 Jefferson Davis Highway, Suite 1204, Arlington, VA 22202-4302, and to the Office of Management and Budget, Paperwork Reduction Project (0704-0188) Washington DC 20503.

1. AGENCY USE ONLY *(Leave blank)*	2. REPORT DATE March 1996	3.REPORT TYPE AND DATES COVERED Master's Thesis	
4. TITLE AND SUBTITLE Swell Propagation Across a Wide Continental Shelf			5. FUNDING NUMBERS
6. AUTHOR(S) Eric J. Hendrickson			
7. PERFORMING ORGANIZATION NAME(S) AND ADDRESS(ES) Naval Postgraduate School Monterey CA 93943-5000			8. PERFORMING ORGANIZATION REPORT NUMBER
9. SPONSORING/MONITORING AGENCY NAME(S) AND ADDRESS(ES)			10.SPONSORING/MONITORING AGENCY REPORT NUMBER
11. SUPPLEMENTARY NOTES The views expressed in this thesis are those of the author and do not reflect the official policy or position of the Department of Defense or the U.S. Government.			
12a. DISTRIBUTION/AVAILABILITY STATEMENT Approved for public release; distribution is unlimited.			12b. DISTRIBUTION CODE

13. ABSTRACT *(maximum 200 words)*

The effects of wave refraction and damping on swell propagation across a wide continental shelf were examined with data from a transect of bottom pressure recorders extending from the beach to the shelf break near Duck, North Carolina. The observations generally show weak variations in swell energy across the shelf during benign conditions, in qualitative agreement with predictions of a spectral refraction model. Although the predicted ray trajectories are quite sensitive to the irregular shelf bathymetry, the predicted energy variations are surprisingly weak, consistent with the observations. These results indicate that small amplitude swell is not significantly damped on the shelf. However, a large decrease in swell energy levels across the shelf (up to 70%) observed with high-energy incident swell, is not predicted by the energy conserving refraction model. These energy losses are likely caused by bottom friction.

14. SUBJECT TERMS Duck94, Swell Propagation, Swell Dissipation, Refraction Model, Continental Shelf.			15. NUMBER OF PAGES 56
			16.PRICE CODE

17. SECURITY CLASSIFICATION OF REPORT Unclassified	18. SECURITY CLASSIFICATION OF THIS PAGE Unclassified	19. SECURITY CLASSIFICATION OF ABSTRACT Unclassified	20.LIMITATION OF ABSTRACT UL

SWELL PROPAGATION ACROSS A WIDE CONTINENTAL SHELF

Eric J Hendrickson
Lieutenant, United States Navy
B.S., Maine Maritime Academy, 1988

Submitted in partial fulfillment
of the requirements for the degree of

MASTER OF SCIENCE IN PHYSICAL OCEANOGRAPHY

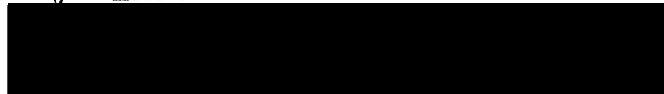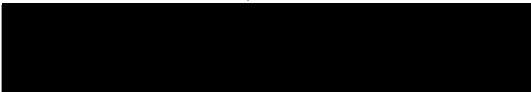from the

NAVAL POSTGRADUATE SCHOOL
March, 1996

Author: _____
Eric J. Hendrickson

Approved by: _____
T. H. C. Herbers, Thesis Advisor

_____
W. C. O'Reilly, Co-Advisor

_____
R. H. Bourke, Chairman
Department of Oceanography

ABSTRACT

The effects of wave refraction and damping on swell propagation across a wide continental shelf were examined with data from a transect of bottom pressure recorders extending from the beach to the shelf break near Duck, North Carolina. The observations generally show weak variations in swell energy across the shelf during benign conditions, in qualitative agreement with predictions of a spectral refraction model. Although the predicted ray trajectories are quite sensitive to the irregular shelf bathymetry, the predicted energy variations are surprisingly weak, consistent with the observations. The results indicate that small amplitude swell is not significantly damped on the shelf. However, a large decrease in swell energy levels across the shelf (up to 70%), observed with high-energy incident swell, is not predicted by the energy conserving refraction model. These energy losses are likely caused by bottom friction.

TABLE OF CONTENTS

LIST OF SYMBOLS

C	phase speed
C_g	group speed
E	shallow water energy spectrum
E_o	deep water energy spectrum
f	frequency
κ	wave number
$\boldsymbol{K}$	energy transformation coefficient
M	directional width parameter
S	distance along a ray
Γ	inverse direction function
Θ	shallow water angle
Θ_o	deep water incidence angle
Θ_{MEAN}	mean propagation direction

x

ACKNOWLEDGEMENTS

I. INTRODUCTION

The propagation of swell over a shallow continental
shelf is a complex process that is still poorly understood.
While swell can traverse ocean basins with very little loss
in energy (Snodgrass et al., 1966), strong spatial
variations in swell energy levels typically occur in shallow
coastal areas. A variety of processes may affect waves as
they propagate across the continental shelf from the open
ocean to the beach. It is well known that refraction and
shoaling strongly affect the coastal wave climate, in
particular in areas with complex bathymetry (Munk and
Arthur, 1951, and O'Reilly; Guza, 1993). Shemdin et al.,
(1980) suggested that bottom friction, percolation through
the bottom and wave-induced bottom motion, all may cause
significant damping of swell propagating across a wide
continental shelf, but the damping rates appear to be
strongly dependent on the sediment type, bottom
microtopography and local currents, all of which are often
unknown. Field measurements show that bottom friction is
sensitive to the presence of small-scale bedforms (Grant and
Madsen, 1986), but wave induced ripples are in constant
transition and extremely difficult to quantify on a natural
sea bed.

Very few measurements of the attenuation of swell in

shallow coastal waters have been reported. Hasselmann et al., (1973) examined the swell attenuation observed during the JONSWAP experiment (1968, 1969) with a 160 km long cross-shore transect of various instruments deployed near Sylt, Germany. The observed strong attenuation of swell did not agree with generally accepted formulations of bottom friction and suggested that bottom damping expressions used in wave prediction models are inaccurate or that other physical processes such as scattering from small scale bottom irregularities cause significant attenuation (Long, 1973).

Young and Gorman (1995) reported similar observations from an array of seven instruments spanning the continental shelf on the southern coast of Australia. Young and Gorman used these measurements in conjunction with the spectral wave model WAM [*WAMDI Group*, 1988] to estimate the contribution of bottom friction to the overall observed decrease in swell energy across the shelf. Although the data analyses span only a period of 18 days at the beginning of the experiment (when most instruments were operational), and only a few of the instruments were in shallow water, Young and Gorman observed significant attenuation of energetic swell across the shelf.

In the present study more extensive observations of the transformation of swell over a continental shelf are presented. A cross-shelf transect of ten internally

recording bottom pressure sensors was deployed offshore of Duck, North Carolina extending seaward from the beach to the shelf break (100 km from shore), between late July and early December 1994. The data set spanned a wide range of wind/wave conditions. During periods of light winds, remotely generated swell with significant wave heights ranging from about 0.1 to 2.5 m were observed.

Swell spectra observed at each of the instrumented sites were compared to predictions of a linear spectral wave transformation model initialized with directional wave data from a National Data Buoy Center (NDBC), 3-m discus buoy located near the seaward end of the transect. A backward ray tracing scheme (O'Reilly and Guza, 1993) was applied to a high resolution (200 m) bathymetry grid to account for refraction effects over the lumpy shelf topography. The discrepancies between the energy conserving model predictions and measured swell energy levels were used to quantify bottom damping effects as a function of the wave conditions.

The experiment, field data and shelf bathymetry are described in Chapter II. The effects of shoaling and refraction on swell transformation across the shelf are illustrated with model simulations in Chapter III. Model/data comparisons are presented in Chapter IV, followed by a summary and conclusions in Chapter V.

3

II. EXPERIMENT AND DATA ANALYSIS

The field data used in this study was collected as part of the DUCK94 Nearshore Processes Experiment conducted offshore of the U.S. Army Corps of Engineers, Coastal Engineering Research Center's, Field Research Facility (FRF) near Duck, North Carolina. The coast consists of a series of relatively straight barrier islands with sandy beaches that are fully exposed to the Atlantic Ocean. The continental shelf is about 100 km wide and only 20 - 50 m deep (Figure 1). The cumulative effect of bottom drag on swell traveling across this wide, shallow shelf may cause a significant reduction in wave heights on the beaches. A transect of wave recorders was deployed on the shelf (Figure 2) to investigate wave propagation and damping.

The instrumentation for the experiment consisted of ten fully self-contained, battery-powered, internally recording bottom pressure sensors deployed along a cross-shelf transect extending from the Duck beach to the shelf break (Figures 1 and 2, the stations are represented by letters). The shallowest instrument X was mounted on a pipe jetted into the beach in 6 m depth just outside the surf zone. At all other sites (depths ranging from 12 - 87 m, Figure 2) the instruments were mounted in the anchor of a surface mooring (Figure 3). Heavy steamer chain was used to decouple the sensitive pressure sensing instrument from the

5

motion of the surface mooring. The instrument package
contains a Setra capacitance type pressure transducer, a
Tattletale microprocessor, and a disk drive for data
storage. Pressure data was recorded nearly continuously
with a 2 Hz sample rate during the four-month-long (August -
November, 1994) deployment. Some malfunctioning data
acquisition systems were replaced with a cassette tape data
storage system utilizing a reduced sampling scheme (one 137
minute long record sampled at 1 Hz every 3 hours). Site B
suffered significant data loss during the first two months
of the experiment, and the shallowest instruments X and A
failed during hurricane Gordon on November 18. The
shallowest site X (6 m depth) and the deepest site I (87 m
depth) were excluded from the present analysis because the
beach was not adequately resolved in the numerical
refraction calculations and high-frequency ($\geq$ 0.1 Hz) swell
is strongly attenuated in 87 m depth.

Measurements of the directional properties of the
incident swell were available from a National Data Buoy
Center (NBDC) 3-m discus buoy located within 2 km of site H.
Although this buoy does not resolve the directional wave
spectrum in detail, the measurements can be used to
characterize a mean swell propagation angle and a
directional spreading factor (O'Reilly et al., 1996).

Surface height spectra were computed from 12-hour-long
bottom pressure records using a linear theory depth

correction. Relatively long (12 hour) data records were
used in the analysis because the travel time of the swell
traversing the shelf is of the order a few hours. Non-
stationary conditions (i.e., temporal variations in spectral
levels of more than 30% over a 12 hour run) were excluded
from the analysis because the model predictions do not
account for time lags in swell arrivals at different sites.
The analysis was restricted to longer period (0.05 - 0.10
Hz) waves which are usually remotely generated and feel the
bottom on the entire shelf. Periods of moderate to strong
winds (speeds > 10 m/s) with possibly significant generation
effects at wave frequencies < 0.10 Hz were also excluded
from the analysis. During the periods of light winds
considered in this study, currents on the shelf were
predominantly tidal with speeds generally less than 50 cm/s
(Haus et al., 1995). The long-period swells considered here
are not significantly affected by shelf currents. The
analysis was further restricted to cases with mean swell
propagation directions (measured near site H) within +/- 35°
from normal incidence to the shelf break (065° $\leq \Theta_o \leq$ 135°).
Observations of larger northerly or southerly swell
incidence angles were excluded because waves approaching the
shelf at large oblique angles are strongly refracted over
the continental slope seaward of the instrumented transect,
and thus the deep water directional properties of these
waves are not well represented by the NDBC buoy measurements

7

collected at the shelf break (site H). After the various rejection criteria were applied, the original data set of 248 observations was reduced to 71 observations.

The observed variability in swell energy levels on the shelf is summarized in Figure 4 with the total swell variances at four sites spanning the shelf. Variation in swell energy across the shelf are generally small (< 30%), with the exception of a single event from julian days 290 to 295. During this time frame when maximum incident swell energy levels occurred at the shelf break (site H), a significant reduction (up to 70%) in energy is observed at the shallower sites.

Accurate predictions of swell refraction requires detailed knowledge of the shelf bathymetry. A high resolution digital bathymetry database was available from the National Ocean Service (NOS), National Geophysical Data Center (NGDC). Unfortunately this data base contained large gaps extending from 36.2° to 36.8° N, and from the beach (75.8° W) to 74.8° W. To fill these gaps, additional bathymetric surveys were conducted during instrument deployment and recovery cruises with a precision depth recorder mounted on the hull of the R/V Cape Hatteras, with a track spacing of order 1 km. The fathometer measurements were detided using sea level data from a tide gauge located near site A on the FRF pier. These corrections are accurate only in the vicinity of the tide gauge (i.e., the inner

8

shelf sites A-C) but the errors (< 0.5 m) are negligibly small compared to the water depths of the mid- and outer-shelf (30-100 m).

Data from the combined NOS and R/V Cape Hatteras surveys was used to create a bathymetry grid for the area 35° N to 38° N and 74° W to 76° W. The North American Datum of 1927 (NAD27) and Mean Low Water (MLW) were used as horizontal and vertical references. Surveys with a World Geodetic System 1984 (WGS84) horizontal grid reference were converted to NAD27 using the Abridged Molodensky Datum Transform Equations (DMA TR8350.2, 1987). A uniform bathymetry grid with six second horizontal resolution ($\approx$200 meter) was obtained from the surveys using the Delaunay tessellation interpolation method of Watson (1982). This method produces a network of near equiangular triangles with the vertices being depth soundings and grid points linearly interpolated from the plane passing through the vertices. A small amount of grid distortion (about 2.5% at the north and south ends of the grid) results from transforming a Mercator projection graticule to Cartesian coordinates. The maximum wave propagation direction errors ($\approx$1°) due to this distortion are negligibly small (O'Reilly and Guza, 1993).

Other potential bathymetric errors that may exist include navigational inaccuracies of survey vessels for the older surveys and temporal changes in shallow water bathymetry due to accretion and erosion of the sandy bottom.

9

These errors are difficult to quantify and may cause significant inaccuracies in the shallow water regions where small changes in depth strongly affect swell propagation.

The North Carolina shelf is characterized by a broad mid-shelf region with multiple ridge-like features that are roughly aligned with the coast line (Figure 1). These ridges with amplitudes of the order 5 m (Figure 2), may contribute significantly to the refraction of low frequency swell propagating across the shelf.

III. SPECTRAL REFRACTION COMPUTATIONS

To quantify the importance of the shelf topography in the observed spatial variations in swell energy, spectral refraction computations were carried out for a wide range of deep water incident wave conditions. The incident wave field was assumed to be stationary and spatially homogeneous, and fully described by a frequency-directional spectrum $E_o(f,\Theta_o)$. The effects of wave generation, nonlinear interactions and dissipation on the shelf were neglected. For a given deep water spectrum $E_o(f,\Theta_o)$ predictions of the transformed spectrum $E(f,\Theta)$ at eight of the instrumented sites A-H (Figure 1) were obtained with a backward ray tracing technique described in O'Reilly and Guza (1991).

From each site rays were traced in all possible directions back to deep water using the ray equations (Munk and Arthur, 1951; LeMéhauté and Wang, 1982):

$$\frac{dX}{dS} = \cos\Theta \qquad (1)$$

$$\frac{dY}{dS} = \sin\Theta \qquad (2)$$

$$\frac{d\Theta}{dS} = \frac{1}{C}\left(\sin\Theta\frac{\partial C}{\partial X} - \cos\Theta\frac{\partial C}{\partial Y}\right) \tag{3}$$

where C is the phase speed, S is distance along a ray and Θ indicates the direction of wave propagation. The horizontal phase speed gradients were calculated using a second degree polynomial fit to the local bathymetry grid, and equations 1-3 were integrated using a 4th order Runge-Kutta method.

Rays were initially computed for all possible shallow water angles Θ at 1° increments and are terminated upon reaching deep water, land or the boundaries of the grid. These angles were subsequently bisected with additional rays until the spacing of the resulting deep water angles Θ_o of adjacent rays was everywhere less than 2.5° (see O'Reilly, 1991, and O'Reilly and Guza, 1991, for further details). The ray trajectories for a given shallow water site yield an estimate of the inverse direction function Γ:

$$\Theta_o = \Gamma(f,\Theta) \tag{4}$$

which defines the deep water incidence angle Θ_o as a function of the frequency f and the shallow water refracted propagation direction Θ (LeMéhauté and Wang, 1982).

Examples of the inverse direction function Γ are shown in Figures 5 and 6. Figure 5 shows the inverse direction functions of sites H (outer-shelf) and C (inner-shelf) for a frequency of 0.10 Hz. At site H (49 m depth), 0.10 Hz swell barely feel the bottom and the Γ function is nearly a 1:1 linear relationship. On the inner shelf (Site C), the cumulative effects of refraction over the wide, lumpy shelf are evident in the sensitivity of the inverse direction function Γ to the shallow water angle Θ. Figure 6 shows the inverse direction functions of sites H and C for 0.07 Hz waves. These lower frequency waves sense the bottom in deeper water and are already significantly refracted at site H. The relatively strong refraction effects noted at site C for southerly deep water angles ($\Theta_o > 150°$) are caused by the curvature of the coast to the south and a group of shoals near Cape Hatteras (Figure 1).

Once the inverse direction function $\Gamma(f,\Theta)$ is evaluated for a given site, the frequency-directional spectrum follows from the transformation relation

$$\frac{E(f,\Theta)}{E_o(f,\Gamma(f,\Theta))} = \frac{\kappa}{\kappa_o} \frac{C_{go}}{C_g} \tag{5}$$

where κ is the wave number, C_g is the group velocity, and subscripts indicate deep water values (Longuet-Higgins, 1957, and LeMéhauté and Wang, 1982). Discritizing the deep

13

water spectrum $E_o(f,\Theta_o)$ in finite frequency-direction bands with widths $(\Delta f, \Delta \Theta_o)$, the energy transformation factor $K(f_i, \Theta_{oj})$ for each band (f_i, Θ_{oj}) follows from integrating (5)

$$K(f_i, \Theta_{oj}) = \frac{1}{\Delta f \, \Delta \Theta_o} \int df \int d\Theta \; \frac{\kappa}{\kappa_o} \frac{C_{go}}{C_g} \qquad (6)$$

where the integration limits include all (f,Θ) rays that terminate within the (f_i, Θ_{oj}) band (i.e., $\left| f - f_i \right| < \Delta f/2$; $\left| \Gamma(f,\Theta) - \Theta_{oj} \right| < \Delta \Theta_o/2$). Finally, predictions of the transformed frequency spectrum $E(f)$ at the instrumented sites are readily computed for any deep water incident wave spectrum $E_o(f,\Theta_o)$ by multiplying E_o by the energy transformation coefficients $\boldsymbol{K}$

$$E(f_i) = \sum_{\Theta_{oj}} K(f_i, \Theta_{oj}) E_o(f_i, \Theta_{oj}) \; \Delta \Theta_o \qquad (7)$$

To investigate the effects of refraction on typical swell arrivals from a single remote source, numerical simulations were carried out with a simple cosine power deep water directional distribution of energy:

$$E_o(\Theta_o) \propto \cos^{2M}\left(\frac{\Theta_o - \Theta_{MEAN}}{2} \right) \qquad (8)$$

14

The mean propagation direction Θ_{MEAN} was varied from 50° to 150° (100° is approximately normal to the shelf) and typical directional width values of M = 25, 50 and 100 were used in the simulations (Figure 7). The swell frequency was varied from 0.05 to 0.10 Hz with a finite bandwidth of 0.01 Hz.

Example model predictions of the transformed swell variance at sites A, C, E, and H (Figure 1) relative to deep water are shown in Figure 8 as a function of Θ_{MEAN}, for f = 0.05, 0.07 and 0.10 Hz, and M = 50. Although the ray trajectories are sensitive to the irregular shelf bathymetry (Figures 5 and 6), the predicted swell energy levels are generally within a factor of 2 of the deep water value and only weakly dependant on Θ_{MEAN}. Not surprisingly, the predicted energy variations on the shelf are very weak for relatively short wavelength 0.10 Hz swell (Figure 8c) and more pronounced for lower frequency waves (Figure 8a,b). It should be noted that very low frequency 0.05 Hz swell (unusual at this site) is significantly affected by refraction before reaching the shelf break (Site H, Figure 8a). For large oblique incidence angles, (<70° and >130°), refraction causes consistent reductions in energy close to shore (e.g., sites A and C).

Small differences (less than 20%) in energy levels predicted at site C for different values of the directional spreading parameter M (25, 50, 100, Figure 9) indicate that the transformation of swell across the shelf is relatively

15

insensitive to the width of the directional spectrum. Overall, the model simulations suggest a weak sensitivity of swell transformation across the shelf to the deep water incident wave conditions.

IV.   MODEL/DATA COMPARISONS

Swell spectra on the shelf estimated from 71 twelve-hour-long data records (the selection of these records is described in Chapter II) are compared here to predictions of an energy-conserving spectral refraction model (described in Chapter III). The model predictions were initialized with directional wave measurements from an NDBC 3-m discus buoy located at the shelf break near site H. Estimates of the directional distributions of incident swell energy in 0.01 Hz wide frequency bands (centered at f = 0.05, 0.06, 0.07, 0.08, 0.09, 0.10 Hz) were extracted from the buoy measurements using the Maximum Entropy Method (Lygre and Krogstad, 1986). These estimates do not resolve the directional spectrum in detail, but, fortunately the refraction model predictions are not overly sensitive to the directional properties of incident swell (Figures 8,9), and mean swell incidence angles are well characterized by the buoy measurements (e.g., O'Reilly et al., 1996). Weak changes in swell propagation directions between deep water and the buoy location (Figures 5,6) were neglected.

To account for small energy variations between site H and deep water owing to shoaling and refraction (note that energy levels at site H can differ significantly from deep water at low swell frequencies, Figure 8) the swell energy spectrum observed at site H was first transformed back to

deep water with Equation 6, and subsequently transformed
across the shelf to all shallower instrumented sites.

Example comparisons of observed and predicted swell
spectra and total variances are shown in Figures 10 - 15
(observed and predicted values are identical at site H,
where the model predictions were initialized). In the
majority of the cases analyzed here, with generally benign
conditions (significant wave heights < 0.5 m), the model
predictions yield a gradual and weak (less than 25% at the
shallowest site) decrease in swell energy levels across the
shelf, in reasonable agreement with the observations (e.g.,
Figures 10 and 11). The agreement of observed and predicted
spectra is sometimes poor at low frequencies where energy
levels are relatively weak (e.g., 0.05 Hz in Figure 10),
possibly owing to inaccuracies in the buoy measurements or
the sensitivity of the refraction model to bathymetry
errors.

In the relatively few observations with energetic swell
(significant wave heights > 1.25 m) a large (up to 70% at
the shallowest site) decrease in spectral levels across the
shelf is observed but not predicted by the refraction model
(Figures 12, 13). The observed attenuation is fairly
uniform over the spectrum (Figure 12) suggesting that the
effects of nonlinear wave-wave interactions are small. The
energy losses are likely caused by bottom friction which is
believed to depend non-linearly on the magnitude of near-

18

bottom velocities (e.g., Grant and Madsen, 1986, and Tolman, 1993).

In some cases with relatively small waves, the refraction model consistently under-predicts swell energy levels at each of the shallower sites (e.g., Figures 14, 15). Similar discrepancies were reported by Young and Gorman (1995) and attributed to spatial variations in deep water incident wave conditions. An alternative explanation for these discrepancies is the limited accuracy of the incident deep water directional information obtained from the NDBC buoy. NDBC buoys are known to over-predict the width of the directional spectrum, in particular with low-energy swell conditions (O'Reilly et al., 1996), and thus cause a bias in the refraction model predictions.

Comparisons of predicted and observed swell variances for all 71 data records are summarized in Figure 16. In most cases predicted and observed variances agree within +/-30% indicating that the damping of swell across the continental shelf (not accounted for by the model predictions)is generally weak. However, during the most energetic swell arrivals (deep water variances > 10^3 cm^2), the energy levels observed at the shallower sites are consistently much lower (up to 70%) than predicted, These large discrepancies suggest that large amplitude swell propagating across a wide shallow shelf is significantly attenuated by bottom friction.

V.   CONCLUSIONS

The effects of wave refraction (due to depth variations) and damping (due to bottom friction) on the propagation of swell across a wide irregular continental shelf were examined with data collected offshore of Duck, North Carolina. A cross-shelf transect of 10 bottom pressure recorders, extending from the beach (6 m depth) to the shelf break (87 m depth), was deployed for a four-month-long period spanning a wide range of conditions. Measurements collected during periods of strong local winds or rapidly changing conditions were discarded to eliminate variability owing to local generation and time lag effects. The remaining data records selected for analysis generally show weak variations in swell energy levels across the shelf during benign conditions, but a strong decrease in energy from the shelf break to the beach when incident swell energy levels were high.

The effects of the irregular shelf bathymetry on the propagation of swell was investigated through simulations with a spectral refraction model for a wide range of incident wave conditions. Although the predicted ray trajectories are quite sensitive to the multiple, ridge-like bathymetric features on the shelf, the predicted energy variations for realistic swell spectra are surprisingly weak. Pronounced refraction effects, evident in a strong

decrease in swell energy across the shelf, are predicted only for large oblique swell incidence angles.

Predictions of the energy conserving refraction model agree reasonably well with the weak variation in swell energy levels observed across the shelf during benign conditions. These comparisons indicate that small amplitude swell is not strongly affected by bottom friction. However, the large decrease in energy levels across the shelf observed with high-energy incident swell is not predicted by the refraction model. This attenuation is likely caused by bottom friction which is believed to depend non-linearly on the magnitude of near bottom velocities.

The model-data comparisons presented here provide only a crude estimate of the importance of bottom damping in the propagation of swell across the continental shelf. The refraction predictions may have significant errors owing to the limited resolution and accuracy of the directional buoy measurements of incident swell. Detailed measurements of incident wave conditions in deep water are needed to obtain quantitative estimates of energy losses owing to bottom friction and other dissipative processes.

APPENDIX

Figure 1. Bathymetry of the North Carolina shelf. The dashed line indicates the instrumented transect. The pressure sensor sites are indicated by letters.

Figure 2. Cross section of the instrumented transect (dashed line in Figure 1). The pressure sensor sites are indicated by letters. (Site D is 7.5 km south of the transect).

Figure 3. Bottom pressure sensor mooring schematic. The instrument package is housed in the anchor and decoupled from the surface buoy motions by shock-absorbing steamer-chain.

Figure 4. Observed swell variability on the shelf for the 71 data runs analyzed in this study. (a) Swell variance at outer shelf site H, (b-d) swell variance at sites E (mid-shelf), C (inner-shelf) and A (nearshore), normalized by the swell variance at site H.

Figure 5. Inverse direction function (Γ) for $f = 0.10$ Hz. Upper panel: Site H (outer shelf). Lower panel: Site C (inner shelf).

Figure 6. Inverse direction function (Γ) for $f = 0.07$ Hz. Upper panel: Site H (outer shelf). Lower panel: Site C (inner shelf).

Figure 7. Cosine power directional distribution for three values of the directional width parameter M.

Figure 8.   Predicted energy relative to deep water versus mean incident wave propagation direction at sites A, C, E and H for f = 0.05, 0.07 and 0.10 Hz and a cosine power directional distribution with width parameter M = 50.

Figure 9.   Predicted energy relative to deep water versus mean incident wave propagation direction at site C for f = 0.07 Hz and a cosine power directional distribution with width parameter M = 25, 50 and 100.

Figure 10.   Predicted (solid curve) and observed (dashed curve) swell spectra at four sites spanning the shelf on 12 September, 1994.

Figure 11.   Predicted and observed swell variance versus distance from shore, on 12 September, 1994.

Figure 12.   Same as Figure 10 for 18 October, 1994.

Figure 13.   Same as Figure 11 for 18 October, 1994.

Figure 14.   Same as Figure 10 for 5 August, 1994.

Figure 15.   Same as Figure 11 for 5 August, 1994.

Figure 16.   Ratio of observed and predicted swell variances at sites E, C and A versus deep water swell variance.

Figure 1

25

Figure 2

26

Surface Buoy

Light weight floats

Sub Surface Buoy

Anchor with Setra
Pressure Sensor

Steamer-Chain

Figure 3

27

Figure 4

28
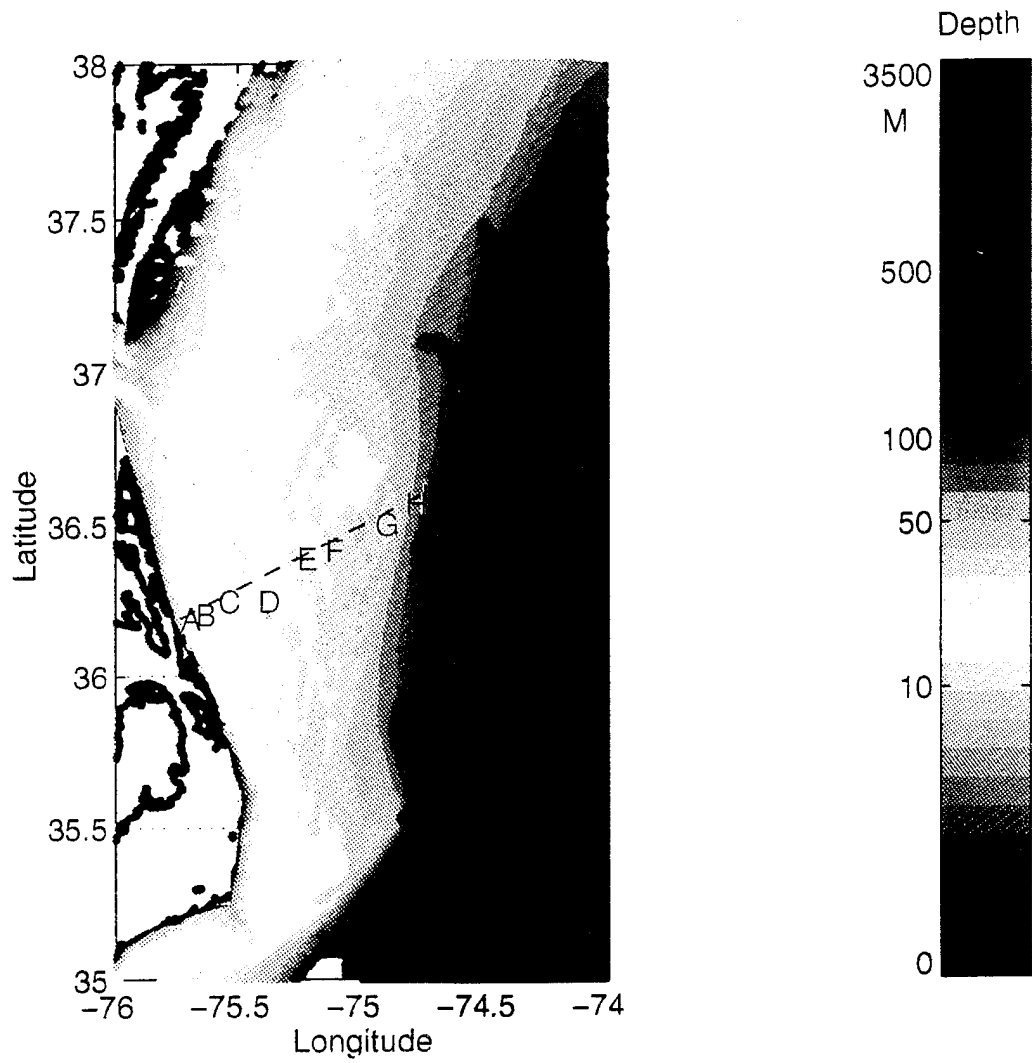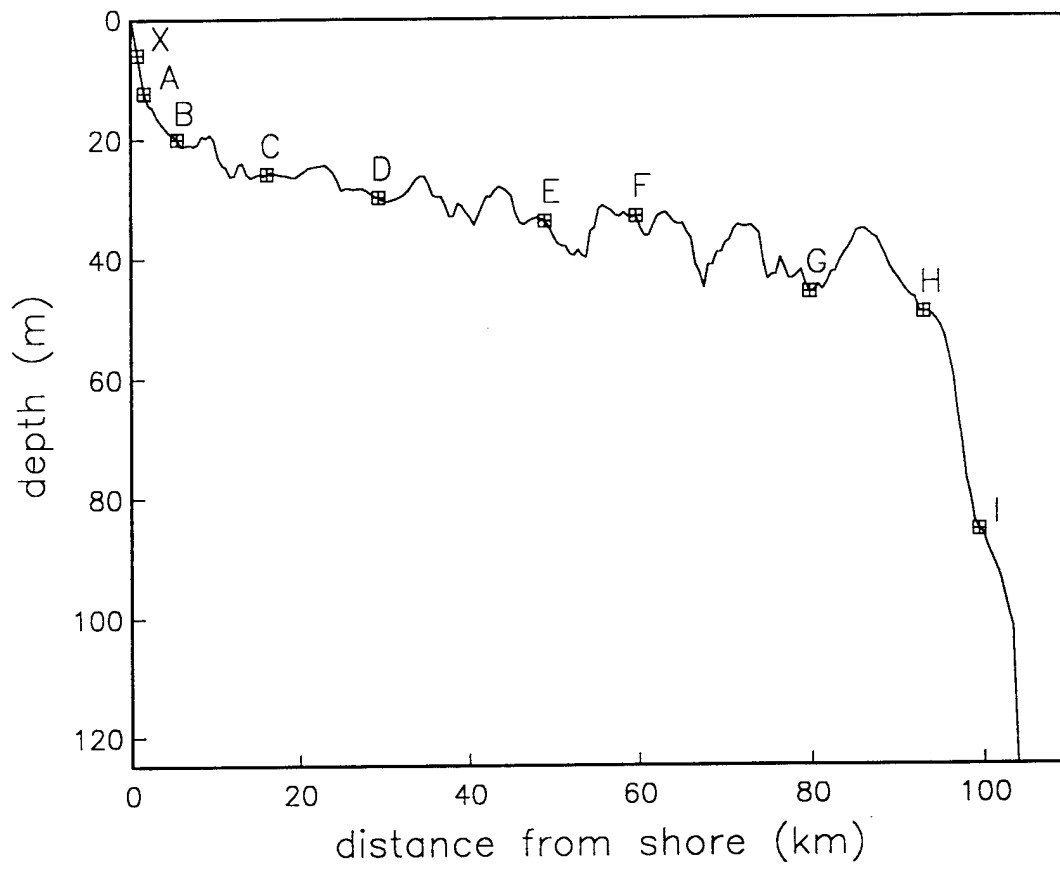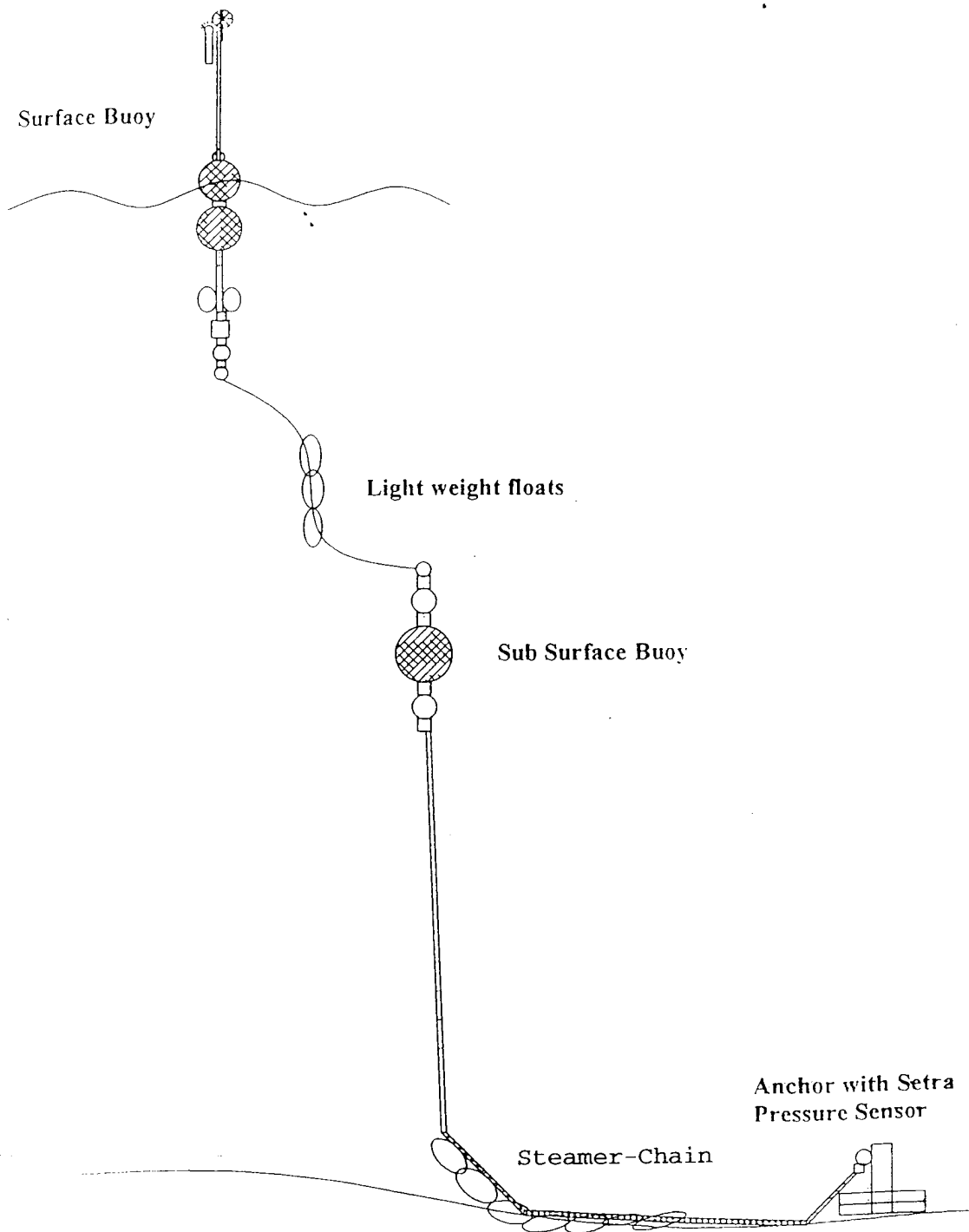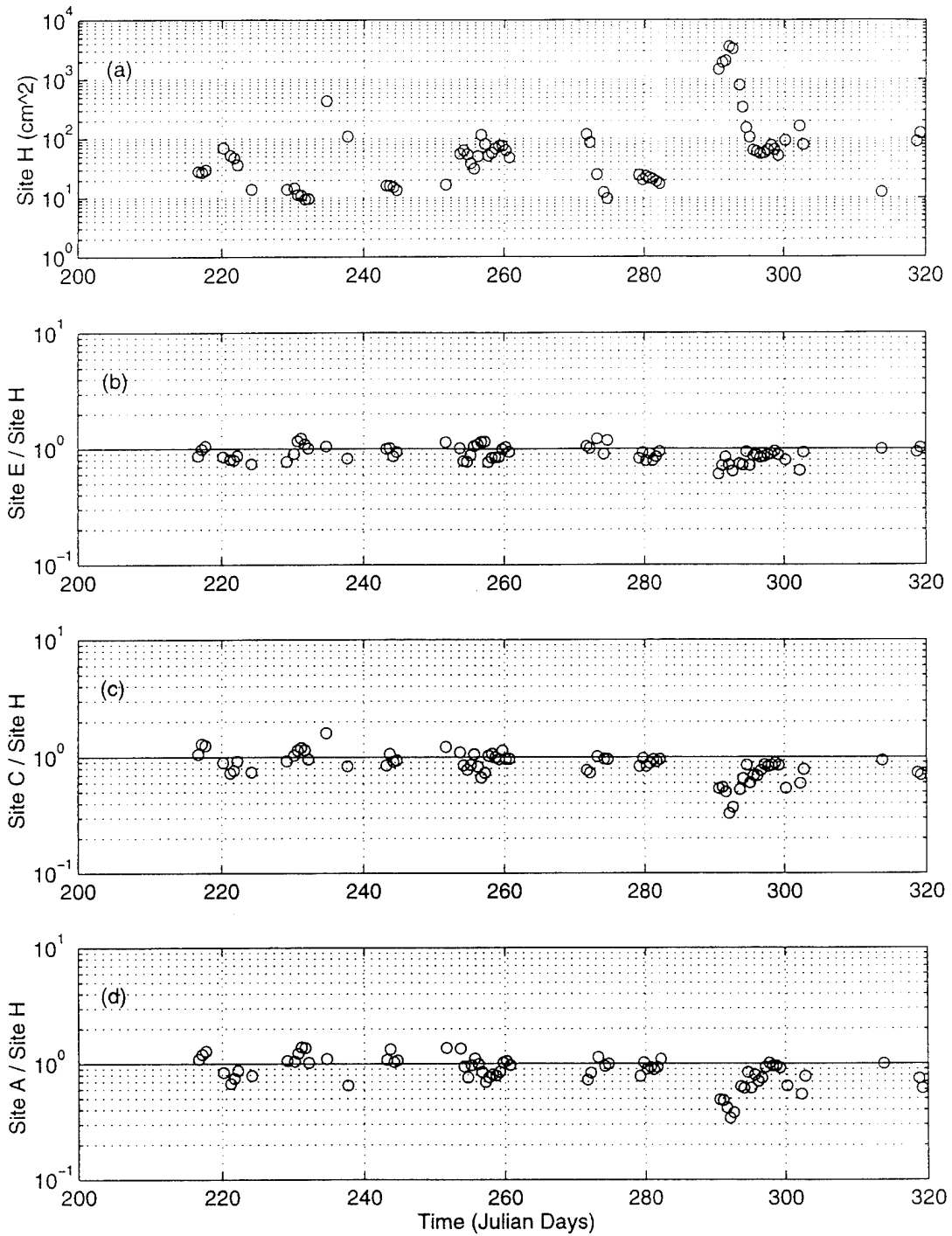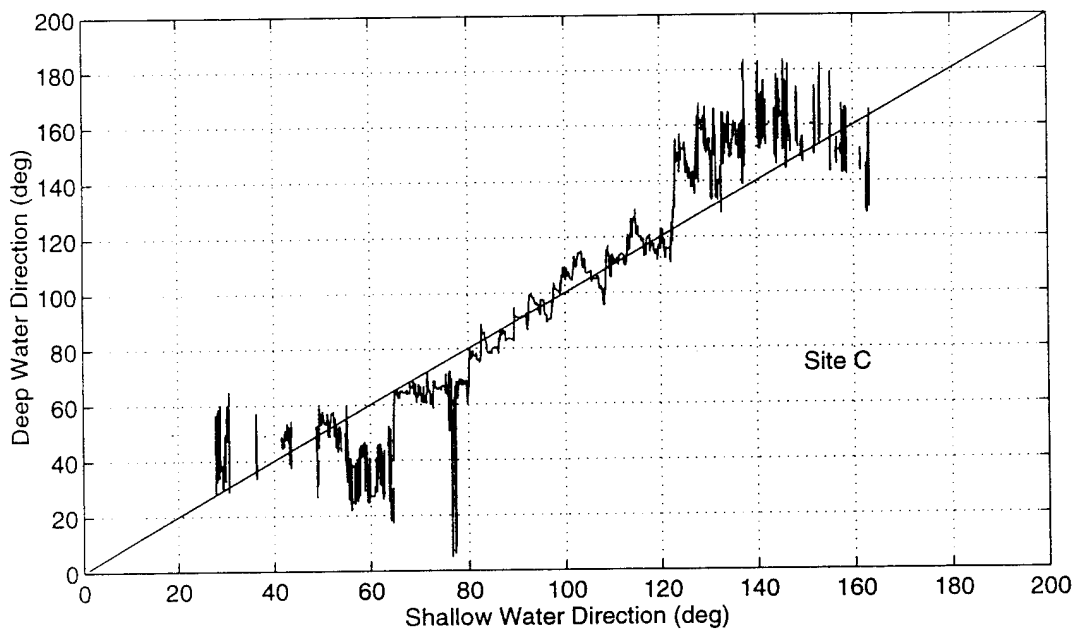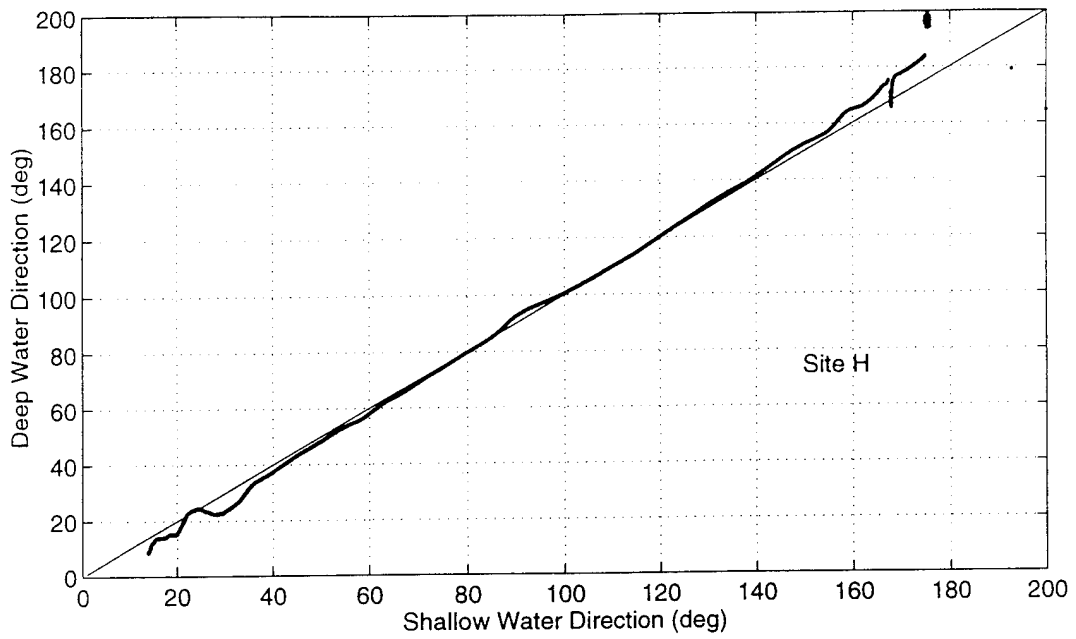
Figure 5

Figure 6

Figure 7

31

Figure 8

32

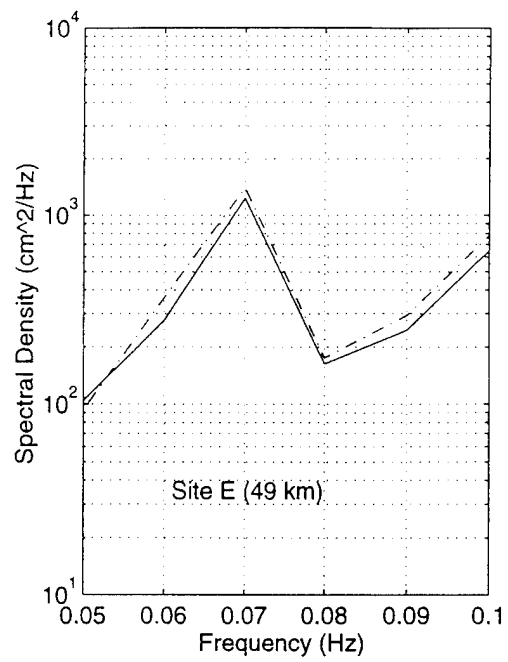Figure 9

33

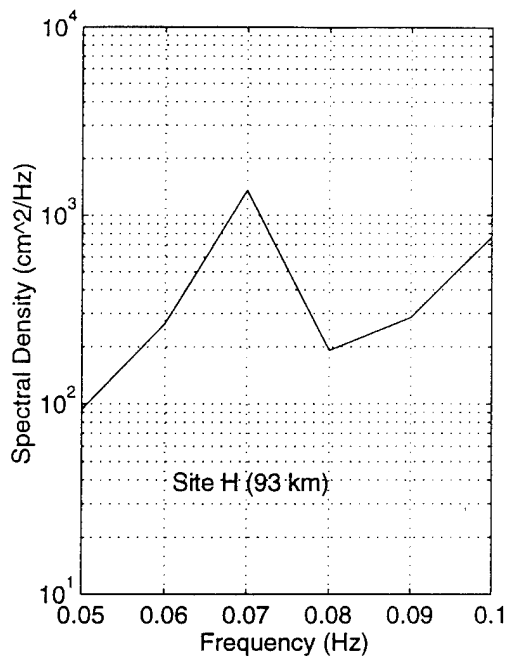Figure 10

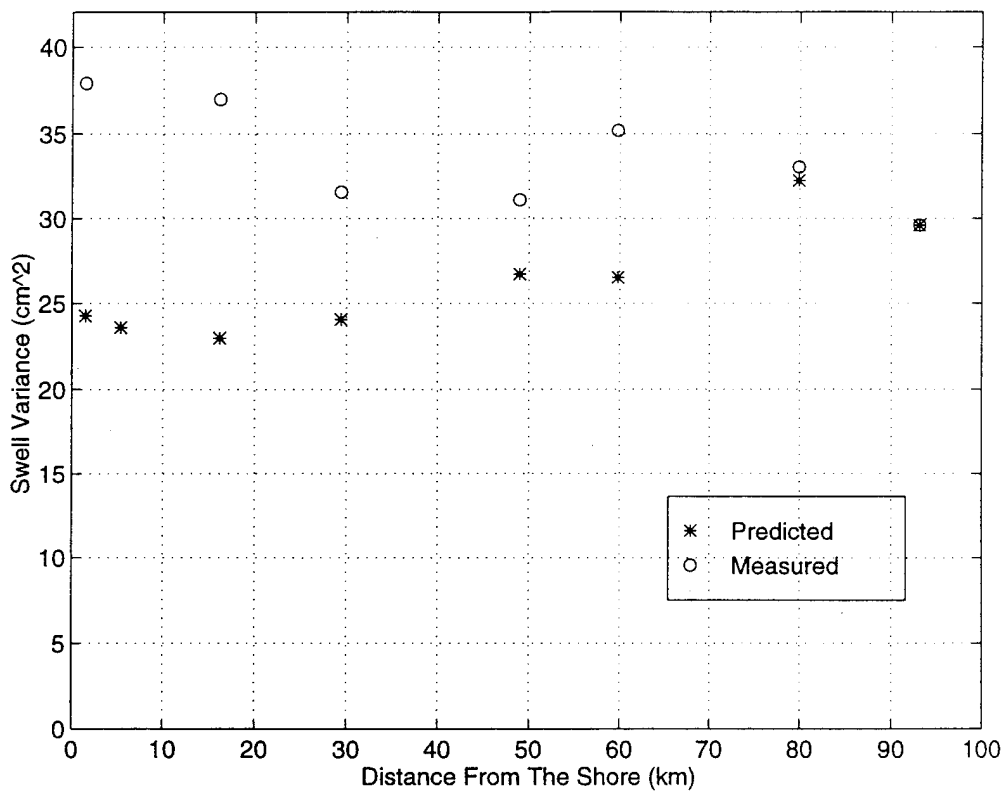34
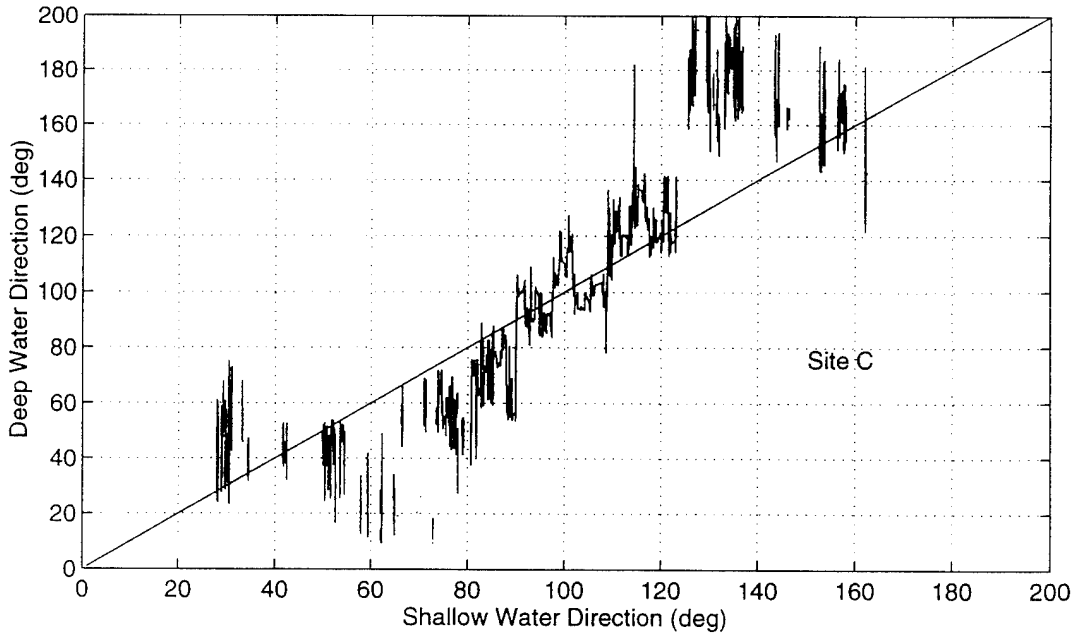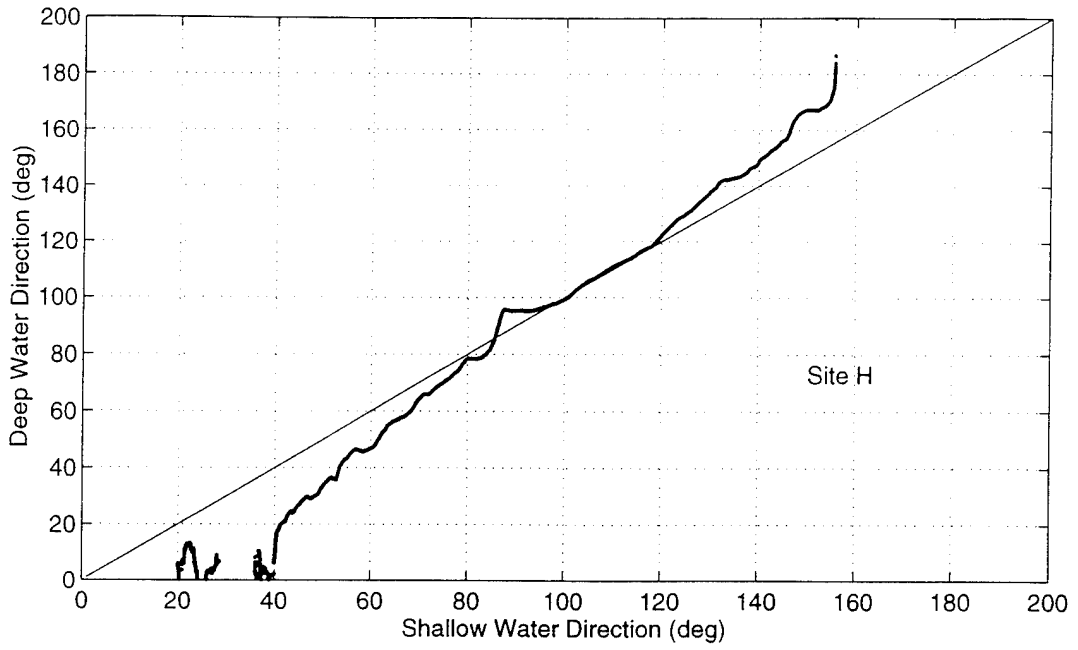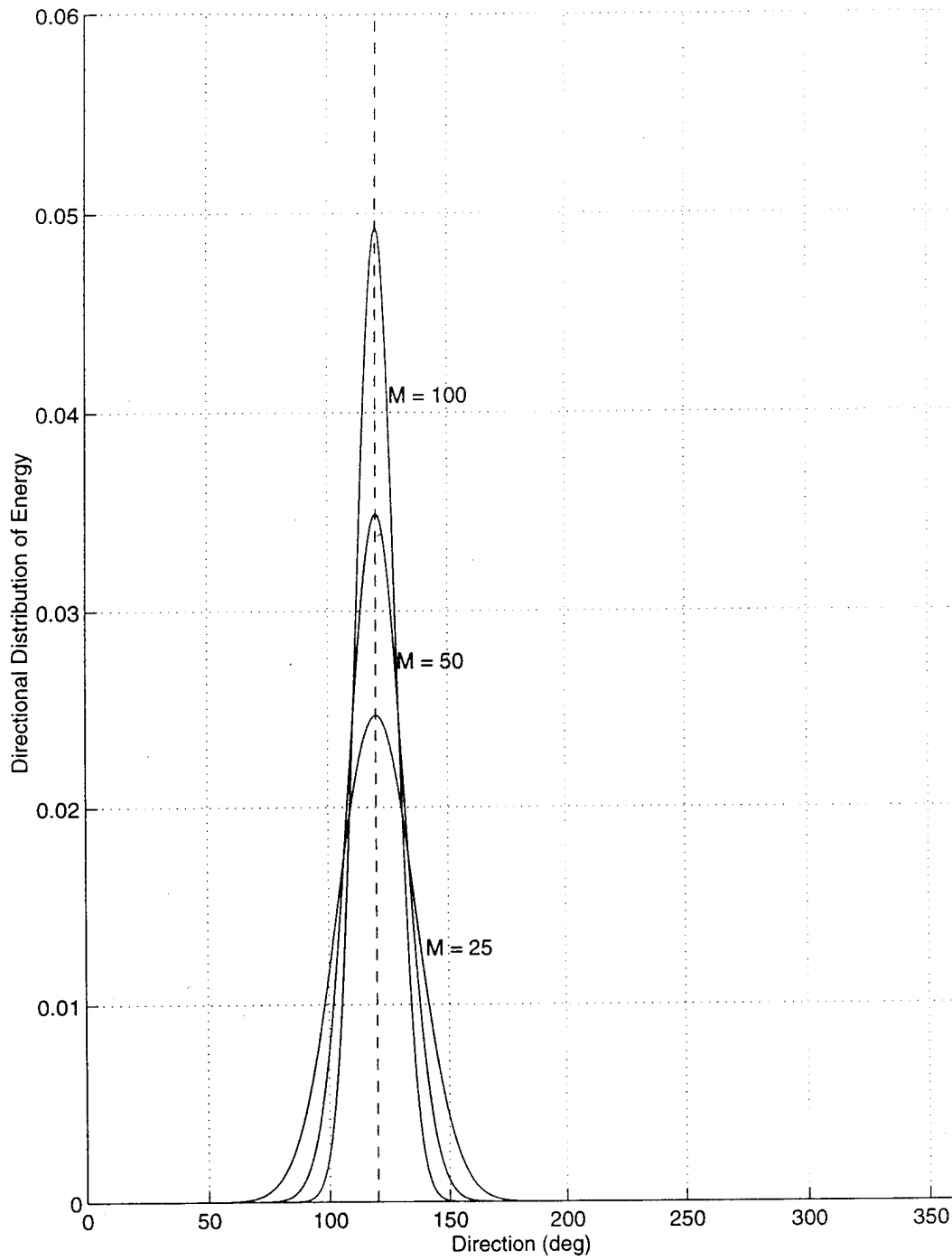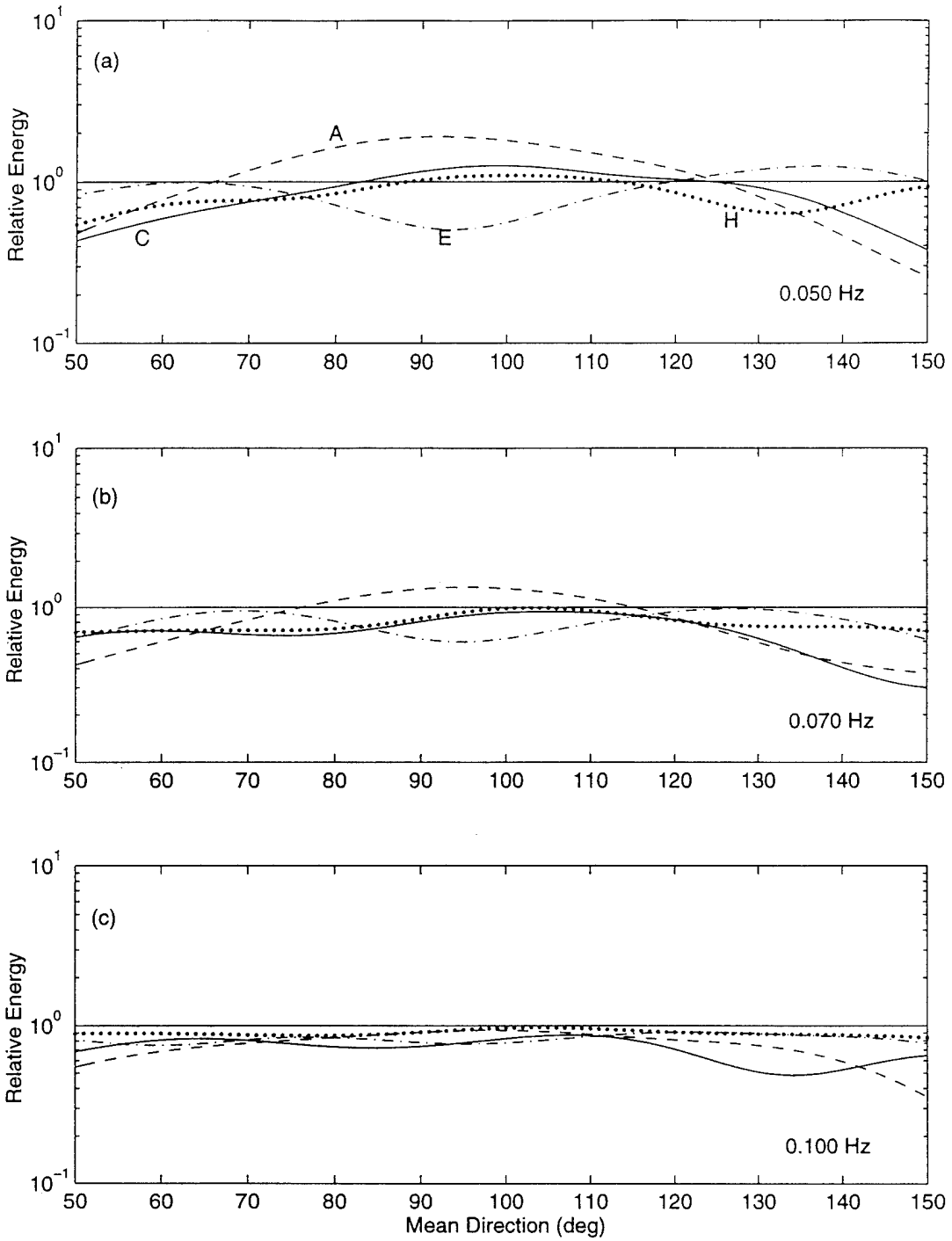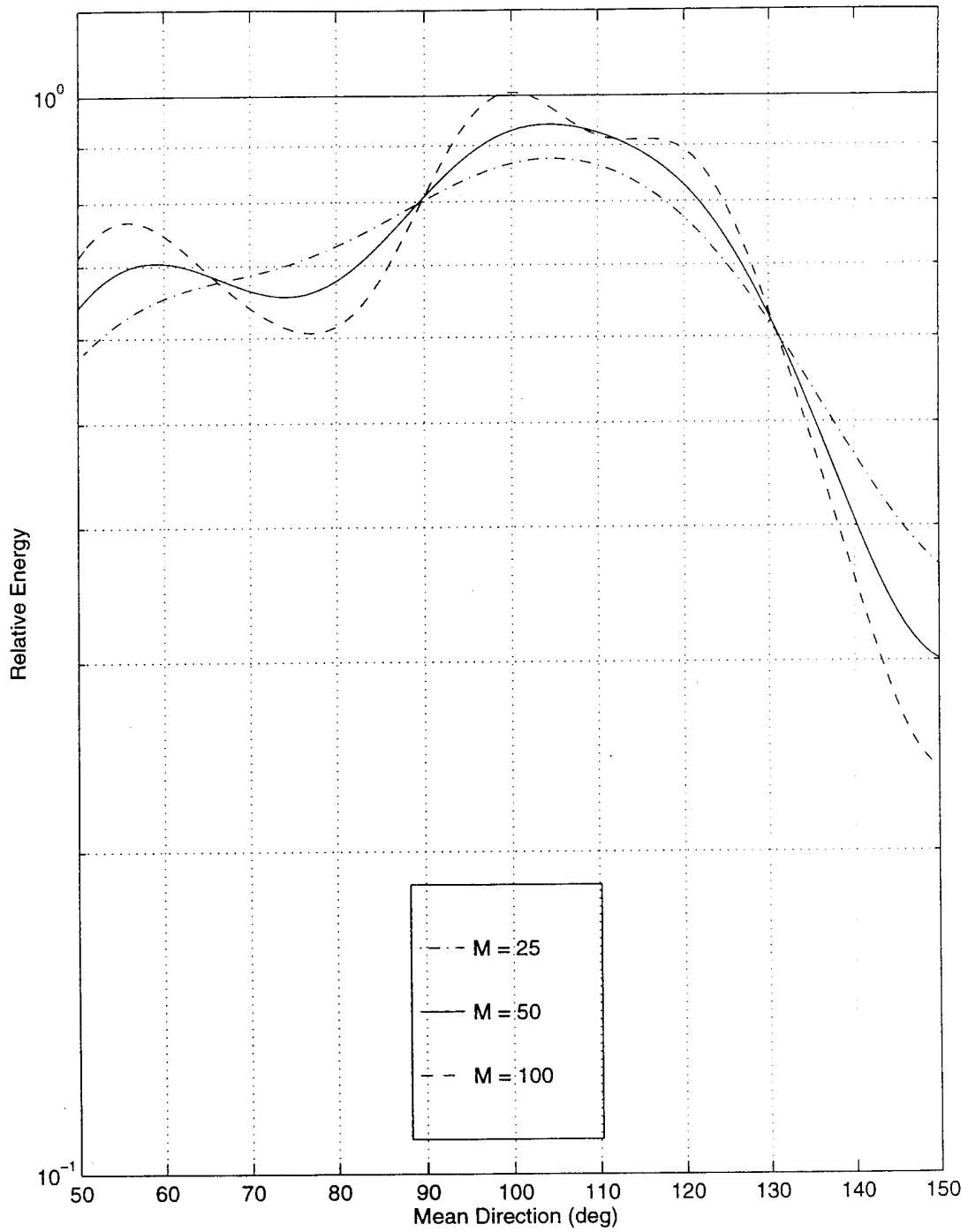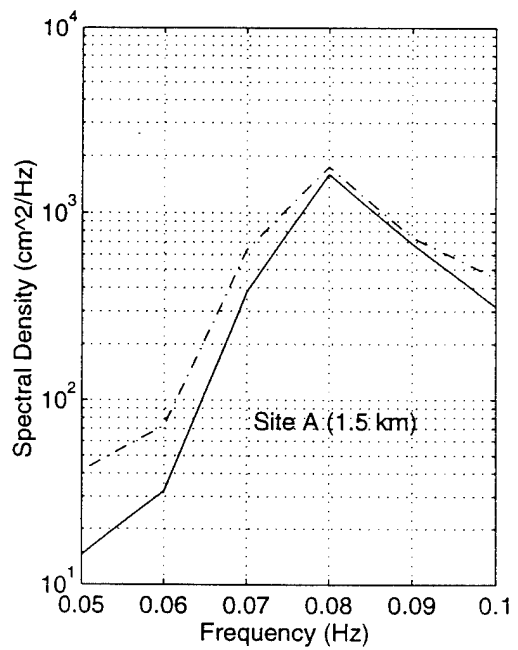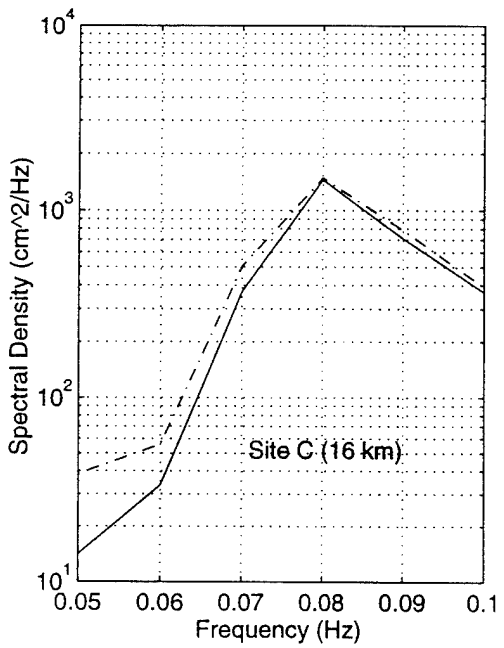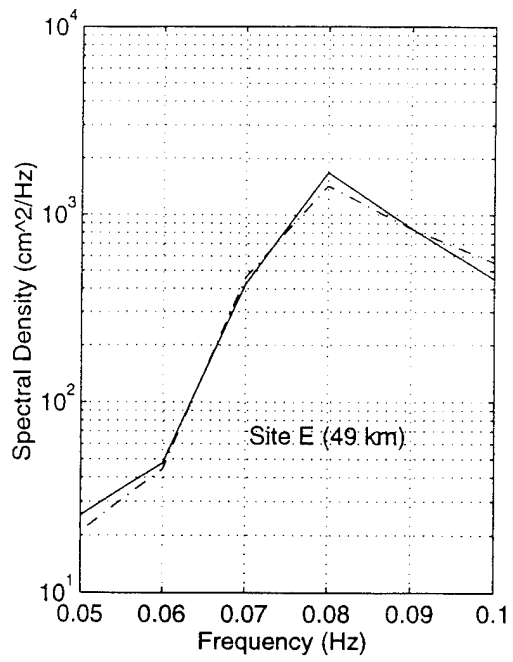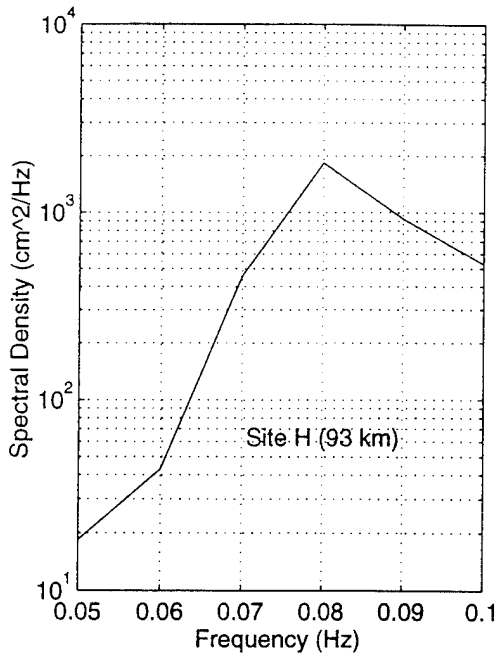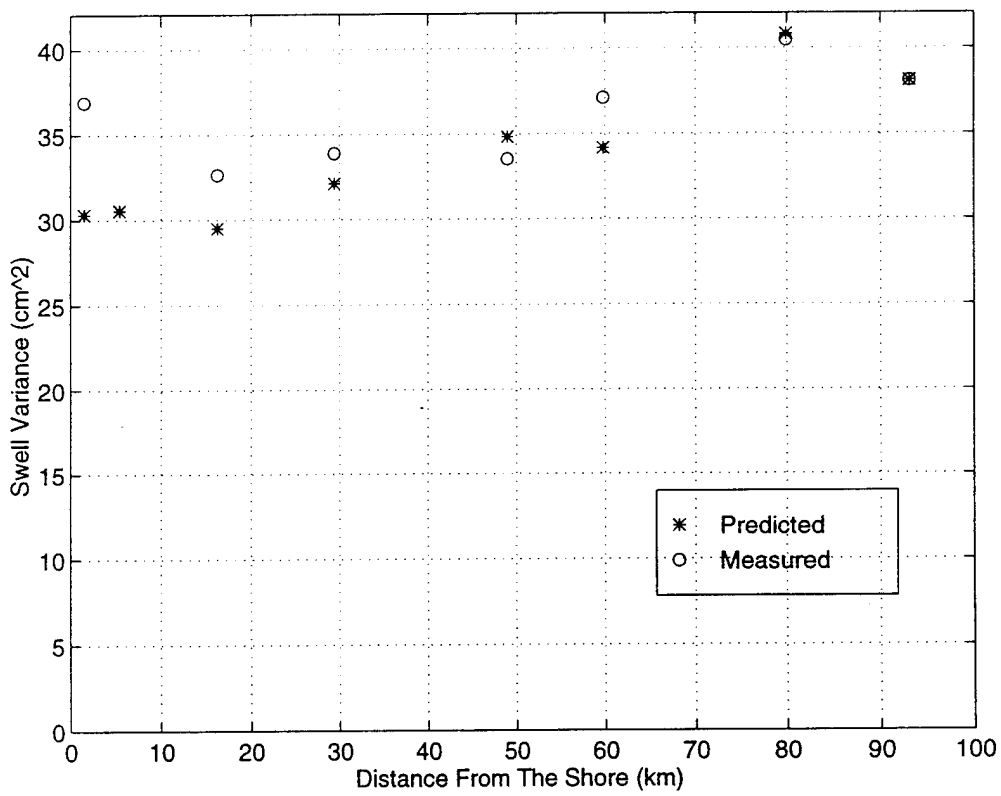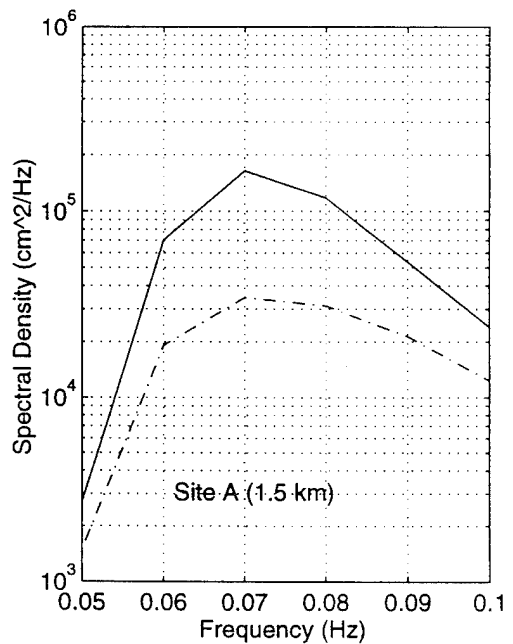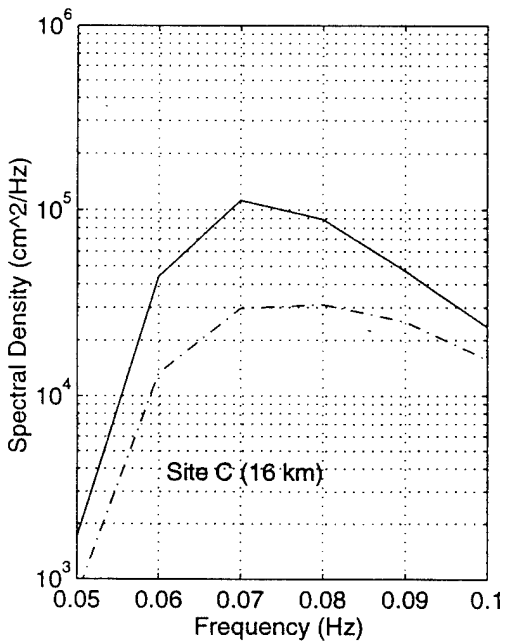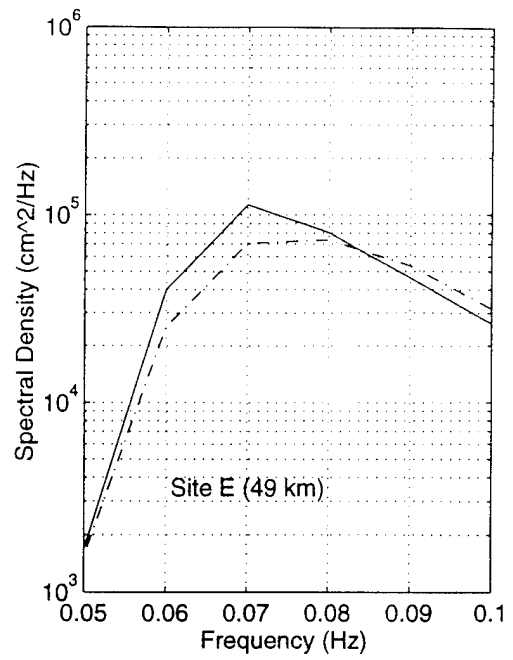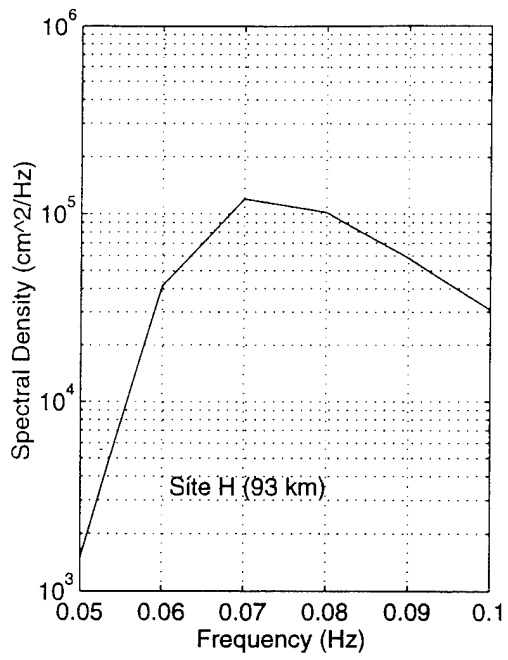
Figure 11
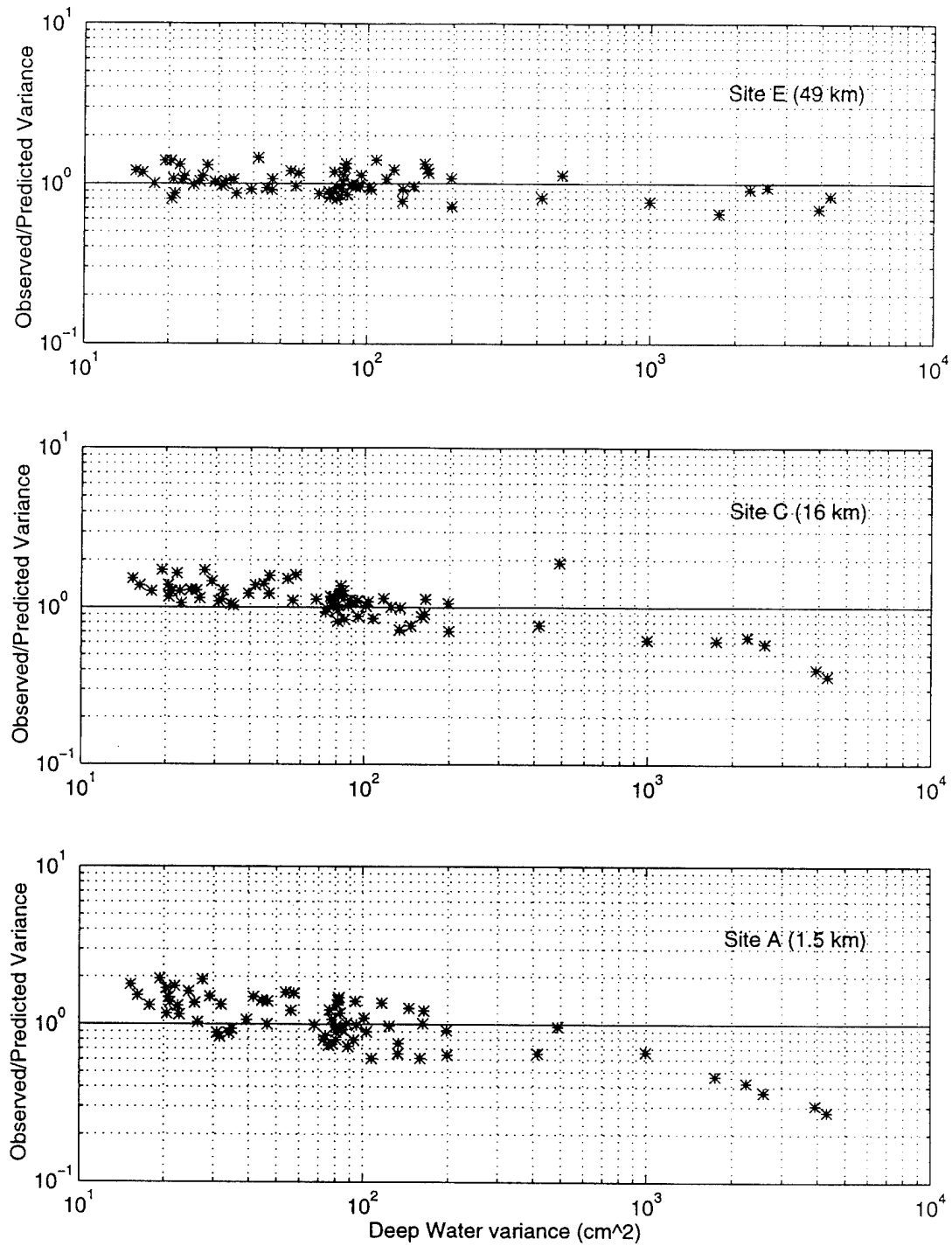
Figure 12

Figure 13

37
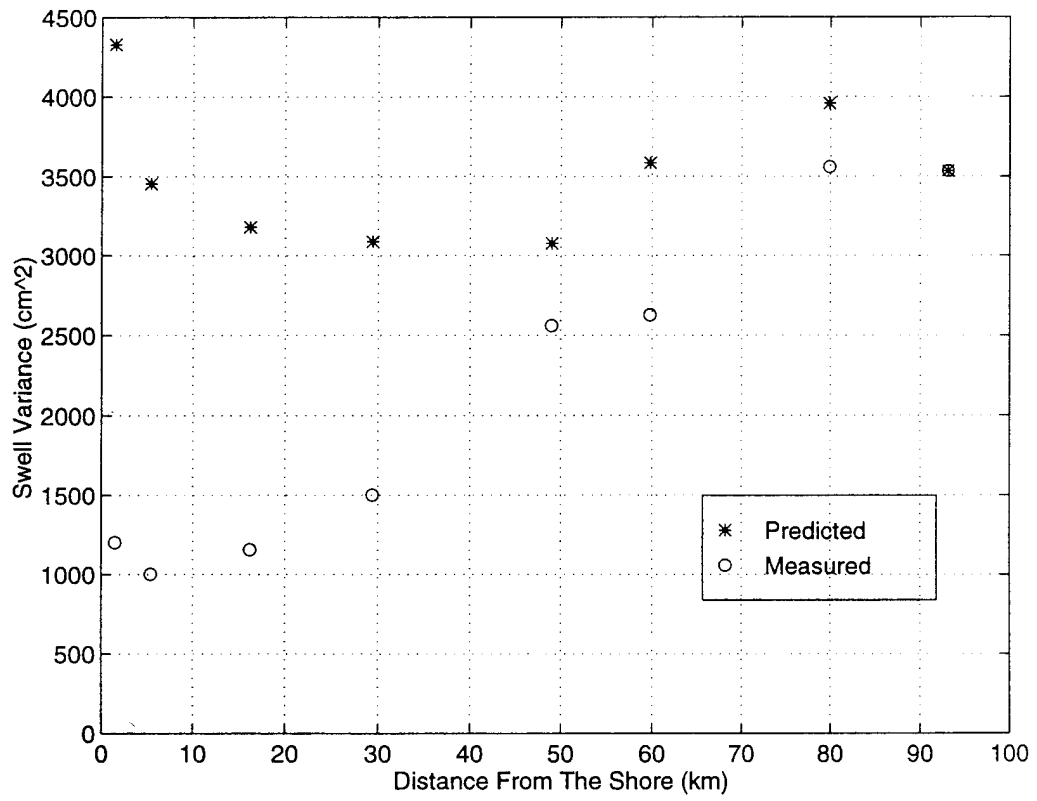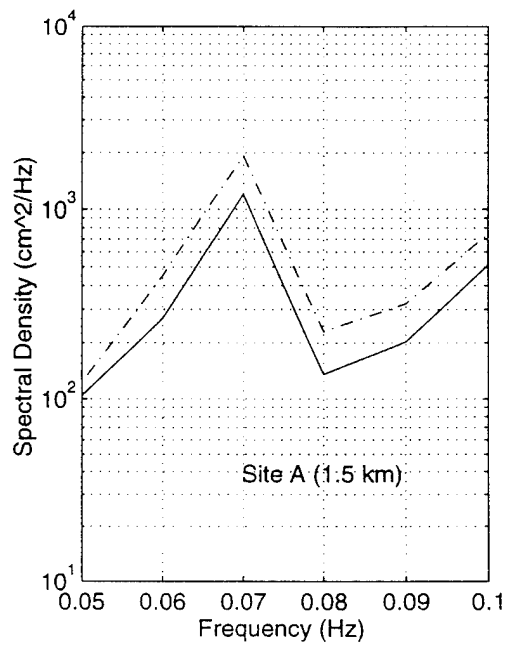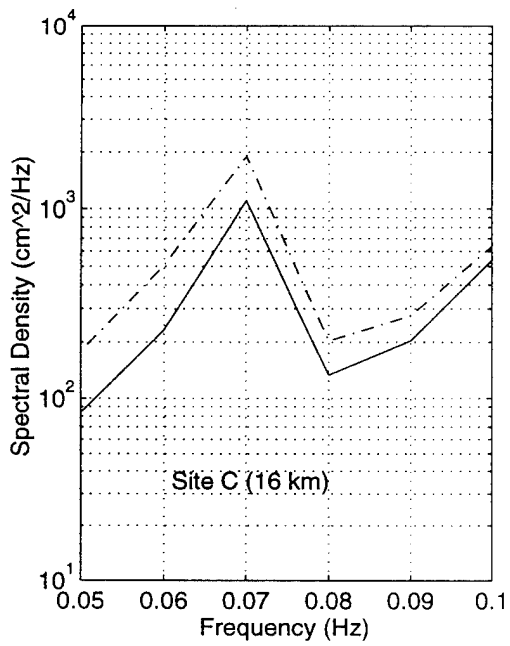
Figure 14

Figure 15

39

Figure 16

LIST OF REFERENCES

DMA Report R,"Department of Defense World Geodetic
    System 1984," DMA, Washington, D.C.

Grant,W.D.,and Madsen,O.S.,1986,"The Continental-Shelf
    Bottom Boundary Layer,"*Ann. Rev. Fluid Mech.*,18,265-
    305.

Hasselmann,K.,T.P.Barnett,E.Bouws,H.Carlsson,D.E.Cartwright,
    K.Enke,J.A.Ewing,H.Gienapp,D.E.Hasselmann,P.Kruseman,A.
    Meerburg,P.Muller,D.J.Oblers,K.Richter,W.Sell,and
    H.Walden,1973,"Measurements of Wind-Wave Growth and
    Swell Decay during the Joint North Sea Wave Project
    (JONSWAP)",*Dtsch. Hydrogr. Z.*,(Suppl.),A,8,12,95pp.

Haus,B.K.,G.C.Graber,L.K.Shay, and J.Martinez,1995,"Ocean
    Surface Current Observations with HF Doppler Radar
    during the DUCK94 Experiment,"Technical Report (RSMAS
    95-010), University of Miami, Miami, FL., 39 pp.

LeMéhauté,B.,and Wang,J.D.,1982,"Wave Spectrum Changes on a
    Sloped Beach,"*J. Waterway, Port, Coastal Ocean
    Eng.*,112(1),78-93.

Long,R.B.,1973,"Scattering of Surface Waves by an Irregular
    Bottom,"*J. Geophys. Res*,78,7861-7870.

Longuet-Higgins,M.S.,1957,"On the Transformation of a
    Continuous Spectrum by Refraction,"*Proc. Cambridge
    Philos. Soc.*,53(1),226-229.

Lygre,A.,and Krogstad,H.E.,1986,"Maximum Entropy Estimation
    of the Directional Distribution in Ocean Wave
    Spectra,"*J. Phys. Oceanogr.*,16(12),2052-2060.

Munk,W.H.,and Arthur,R.S.,1951,"Wave Intensity Along a
    Refracted Ray,"*Circular 521,Gravity Waves, National
    Bureau of Standards*,95-108.

O'Reilly,W.C.,1991,"Modeling Surface Gravity Waves in the
    Southern California Bight,"Ph.D. Dissertation,Univ. of
    California. San Diego,90pp.

O'Reilly,W.C.,and Guza,R.T.,1991,"Comparison Spectral
    Refraction and Refraction-Diffraction Wave Models,"*J.
    Waterway, Port, Coastal Ocean Eng.*,177(3),199-215.

_____and_____,1993,"A Comparison of Two Spectral Wave Models in the Southern California Bight,"*Coastal Engineering*,19,263-282.

O'Reilly,W.C.,T.H.C.Herbers,R.J.Seymour,and R.T.Guza,1996,"A Comparison of Directional Buoy and Fixed Platform Measurements of Pacific Swell,"*J. Atmos. Oceanic Technol.*,13,231-238.

Snodgrass,F.E.,G.W.Groves,K.F.Hasselmann,G.R.Miller,W.H.Munk and W.H.Powers,1966,"Propagation of Ocean Swell Across the Pacific," *Philos. Trans. R. Soc. London*, A, 259,431-497.

Tolman,H.L.,1994,"Wind Waves and Moveable-Bed Bottom Friction,"*J. Phys. Oceanogr.*,24,994-1009.

WAMDI Group,1988,"The WAM model - A Third Generation Ocean Wave Prediction Model,"*J. Phys. Oceanogr.*,18,1775-1810.

Watson,D.F.,1982,"ACORD:Automatic Contouring of Raw data,"*Comput. Geosci.*,8(1),97-101.

Young,I.R.,and Gorman,R.M.,1995,"Measurements of the Evolution of Ocean Wave Spectra Due to Bottom Friction,"*J. Geophys. Res.*,100(C6),10,987-11,004.

INITIAL DISTRIBUTION LIST

1. Defense Technical Information Center   2
    8725 John J Kingman Rd., STE 0944
    Ft. Belvoir, VA 22060-6218

2. Dudley Knox Library   2
    Naval Postgraduate School
    411 Dyer Rd.
    Monterey, CA 93943-5101

3. Dr. T.H.C. Herbers, Code Oc/He   10
    Department of Oceanography
    Naval Postgraduate School
    Monterey, CA 93943-5101

4. Dr. W.C. O'Reilly   2
    412A O'Brien Hall
    University of California, Berkeley
    Berkeley, CA 94720

5. Dr. E.B. Thornton, Code Oc/Tm   1
    Department of Oceanography
    Naval Postgraduate School
    Monterey, CA 93943-5121

6. P.F. Jessen, Code Oc/Js   1
    Department of Oceanography
    Naval Postgraduate School
    Monterey, CA 93943-5121

7. LT E.J. Hendrickson, USN   2
    V-2
    USS Eisenhower CVN-69
    FPO. AE 09532-2830